Dalton Transactions

PAPER

View Article Online
View Journal | View Issue

Cite this: *Dalton Trans.*, 2015, **44**, 15279

Liquid-phase step-by-step growth of an iron cyanide coordination framework on $LiCoO_2$ particle surfaces†

Rie Makiura,*‡[a,b] Shingo Teragawa,[c] Kohei Tsuchiyama,[a] Akitoshi Hayashi,[c] Kiyoharu Tadanaga§[c] and Masahiro Tatsumisago[c]

Received 11th March 2015,
Accepted 12th May 2015

DOI: 10.1039/c5dt00968e

www.rsc.org/dalton

Surface modification of inorganic objects with metal–organic frameworks (MOFs) – organic–inorganic hybrid framework materials with infinite networks – opens wide windows for potential applications. In order to derive a target property, the key is the ability to fine tune the degree of modification. Solution-based step-by-step growth techniques provide excellent control of layer thickness which can be varied with the number of deposition cycles. Such techniques with MOFs have been mainly applied to flat substrates, but not to particle surfaces before. Here, we present the facile surface modification of inorganic particles with a framework compound under operationally simple ambient conditions. A solution-based sequential technique involving the alternate immersion of $LiCoO_2$ (LCO) – a positive electrode material for a lithium ion battery – into $FeCl_2{\cdot}4H_2O$ and $K_3[Fe(CN)_6]$ solutions results in the formation of Prussian blue (PB) nanolayers on the surface of the LCO particles (PBNL@LCO). The PB growth is finely controlled by the number of immersion cycles. An electrochemical cell with PBNL@LCO as a positive electrode material exhibits a discharge capacity close to the specific capacity of LCO. The results open a new direction for creating suitable interfacial conditions between electrode materials and electrolytes in secondary battery materials.

Introduction

Lithium ion batteries have been widely used not only for portable electrical products, but also for vehicles and industrial heavy machineries.[1] $LiCoO_2$ (LCO) is the most popular practical positive electrode material because it can be easily synthesized and shows reasonable charge–discharge capacity.[2] On the other hand, extensive delithiation increases the electrostatic repulsion between adjacent CoO_2 layers and causes irreversible structural deformation of LCO as well as decomposition of the electrolytes on the electrode surfaces. Improvement of the cyclability has been demonstrated by coating the LCO surface with a thin layer of a variety of oxides such as Al_2O_3,[3a] TiO_2,[3b] ZrO_2,[3c] Li_2SiO_3,[3d] Co_3O_4,[3e] B_2O_3,[3f] MgO,[3g] and ZnO.[3h] The coated oxides contribute to the enhancement of the structural stability of the core LCO surface. In addition, the interfacial reaction between the positive electrode materials and electrolytes is suppressed in the presence of the inert oxides. Furthermore, in order to improve the contact between electrode active materials and solid electrolytes in all-solid battery systems, in which such solid–solid interfacial contact area is generally much smaller than that of solid–liquid interfaces in conventional battery systems composed of liquid electrolytes, coating of the LCO particle surfaces with electrolyte materials has also been reported.[4]

Organic–inorganic hybrid framework materials with infinite networks including porous compounds so-called metal–organic frameworks (MOF) or porous coordination polymers (PCP) have been attracting great interest because of the rich variety of materials as well as their diverse chemical/physical properties.[5] The mixed-valence iron cyanide system, $Fe_4[Fe(CN)_6]_3{\cdot}xH_2O$ called Prussian blue (PB) is a well-known framework compound, which has been studied extensively for its unique electrochromic and magnetic behavior together with its analogues (PBAs).[6] PB and PBAs have been recently examined as positive electrode materials for lithium secondary bat-

[a]*Nanoscience and Nanotechnology Research Center, Research Organization for the 21st Century, Osaka Prefecture University, Sakai, Osaka, Japan.*
E-mail: r-makiura@mtr.osakafu-u.ac.jp
[b]*PRESTO, Japan Science and Technology Agency, Saitama, Japan*
[c]*Department of Applied Chemistry, Graduate School of Engineering, Osaka Prefecture University, Sakai, Osaka, Japan*

†Electronic supplementary information (ESI) available: SEM images of the PBNL@LCO particles before and after immersion into the liquid electrolyte. See DOI: 10.1039/c5dt00968e

‡Present address: Department of Materials Science, Graduate School of Engineering, Osaka Prefecture University, Sakai, Osaka, Japan.
§Present address: Division of Materials Chemistry, Faculty of Engineering, Hokkaido University, Sapporo, Japan.

teries, showing high cyclability attributed to highly reversible alkali metal intercalation and deintercalation without any structural transition or deformation because of their stable three-dimensional network structures.[7]

Representative oxide coating procedures on the LCO active materials include both wet (precipitation and sol–gel) and dry (vacuum deposition) processes.[3] An important issue for such surface coating treatments is the fine control of the thickness of the coating materials at the nanoscale as they may work negatively by interrupting smooth intercalation–deintercalation and by increasing the internal cell resistance if the thickness is not appropriate. On the other hand, PB and PBAs can be prepared as thin homogeneous films on a flat substrate by a sequential deposition technique.[8] Similarly other hybrid framework materials including MOFs can also be prepared in a highly-crystalline thin film state by a solution-based bottom-up approach.[9] The merit of this technique is that it allows excellent tuning of the film thickness as it can be easily controlled by the number of deposition cycles. We consider that PBAs are highly promising candidates as surface coating materials because of their high structural stability[7] and the facile applicability of sequential techniques to their growth.[8] Although composites of MOFs and inorganic nanoparticles such as Au,[10] Co,[11] SiO_2,[12] Fe_2O_3 [13] and $Zn_3(PO_4)_2{\cdot}4H_2O$[14] have been reported,[15] there have been no reports on employing hybrid framework materials including PBAs as surface modification compounds for metal-oxide positive electrode materials of rechargeable batteries. Here, we demonstrate how the step-by-step sequential growth of PB can be adeptly applied in particle surface modification of a positive electrode material in an electrochemical cell.

Experimental

Sequential surface coating of $LiCoO_2$ with Prussian blue (PBNL@LCO)

3 g of $LiCoO_2$ (LCO, Toda Kogyo Corp., the Brunauer–Emmett–Teller (BET) surface is 0.12 $m^2\ g^{-1}$), **1**, was dispersed into 50 mL of ethanol. 250 mL of 10 mM isonicotinic acid (Tokyo Chemical Industry Co., Ltd), **2**, ethanol solution was added into the LCO dispersed solution and the solution was kept stirring for 1 hour. The LCO dispersed in the isonicotinic acid solution was filtered and washed with ethanol, and dried in air. The following two procedures, (i) and (ii), were then conducted. (i) The isonicotinic acid attached LCO particles were added into 300 mL of 10 mM $FeCl_2{\cdot}4H_2O$ (Kanto Chemical Co., Inc.), **3**, aqueous solution. The solution was kept stirring for 10 minutes and filtered. In order to remove excess of **3**, the collected LCO particles were washed by adding into 300 mL of purified water under stirring and filtered. The water wash/filtering procedure was repeated twice. (ii) The collected LCO particles were added into 300 mL of 10 mM $K_3[Fe(CN)_6]$ (Kanto Chemical Co., Inc.), **4**, aqueous solution. The LCO dispersion was kept stirring for 10 minutes. In order to remove excess of **4**, the collected LCO particles were washed by adding into 300 mL of purified water under stirring and filtered. The water wash/filtering procedure was repeated twice. The set of procedures (i) and (ii) is counted as a single cycle and we repeated it up to nine times. The LCO particles coated with Prussian blue nanolayers (PBNL@LCO) were dried at 60 °C under air for three hours and under vacuum for one night. For further removal of adsorbed water in the PBNL@LCO sample, the sample was heated at 140 °C under Ar. We confirmed with IR absorption spectroscopy that the PB framework was not decomposed by the heat treatment.

Infrared (IR) absorption spectroscopy

IR absorption spectra of the PBNL@LCO samples were collected with a Jasco FT-IR/620 Fourier Transform Infrared Spectrometer at room temperature under vacuum conditions. All spectra were recorded with a 4 cm^{-1} resolution.

Scanning electron microscope (SEM)

Morphology of the PBNL@LCO samples was observed by a scanning electron microscope (SEM, JSM-6610A, JEOL) equipped with an energy dispersive X-ray spectroscopy system (EDX, JED-2300, JEOL).

Impedance spectroscopy

Electric conductivity data of the PBNL@LCO samples were collected by AC impedance measurements using an impedance analyzer Solartron 1260 in the frequency range from 10 Hz to 1 MHz. The measurements were conducted with pelletized samples of 10 mm in diameter and about 0.3 mm in thickness. The pellet samples were prepared by applying a uniaxial pressure of 370 MPa for five minutes at room temperature and stainless steel plates were used as current collectors.

Electrochemical characterization

Electrochemical cells were fabricated using PBNL@LCO as a positive electrode active material. PBNL@LCO was mixed with acetylene black and polyvinylidene difluoride (PVDF) solution (8 wt% in *N*-methylpyrrolidone) using an agate mortar (weight ratio for PBNL@LCO : acetylene black : PVDF = 90 : 5 : 5). The mixture was applied on the surface of an aluminium (Al) mesh (The Nilaco Co.) and dried at 130 °C for three hours under Ar. The mixture on the Al mesh was pressed by applying a pressure of 370 MPa for one minute and used as a positive (working) electrode. A lithium (Li) foil (0.25 mm, Furuuchi Chemical Co.) attached on a nickel (Ni) mesh (0.25 mm, The Nilaco Co.) was used as a counter electrode. Another Li foil on the Ni mesh was prepared as a reference electrode. 1 M $LiPF_6$ in ethylene carbonate (EC)–diethyl carbonate (DEC) solvent (1/1 vol%/vol%, Tomiyama Pure Chemical Industries Ltd, LIPASTE-EDEC/PF1) was used as an electrolyte. All cell preparation procedures were performed in a dry Ar-filled glove box. Electrochemical tests were conducted at a constant current density of 0.1 mA cm^{-2} in the voltage range from 2.6 to 4.2 V at 25 °C under an Ar atmosphere using a charge–discharge measurement device.

Results and discussion

Step-by-step surface modification and characterization

The deposition procedure is initiated by the surface treatment of lithium cobalt oxide, $LiCoO_2$ (LCO) particles, **1**, with isonicotinic acid, **2**, which works as an adhesive layer – the carboxylic groups attach to the LCO surface while the pyridyl parts allow subsequent introduction of iron ions *via* coordinative bonding, as schematically shown in Fig. 1. After rinsing excess physisorbed isonicotinic acid with ethanol, the coated LCO particles are alternately immersed into aqueous solutions of $FeCl_2{\cdot}4H_2O$, **3**, and $K_3[Fe(CN)_6]$, **4**. This sequential step-by-step procedure, which includes intermediate solvent (water) immersion and room temperature drying steps, results in the generation of PB nanolayers (PBNL) on the LCO particle surface (PBNL@LCO).

The successful step-by-step framework growth of PBNL was followed by infrared (IR) absorption spectroscopy (Fig. 2). The evolution of the characteristic T_{1u} stretching vibration of the bridging cyanide ions in PBNL at ~2050 cm^{-1} was monitored as a function of the number of coating cycles (Fig. 2a). The continuous growth of the absorbance, as shown in Fig. 2b, provides evidence that PBNL grows in a sequential manner on the LCO particle surface.

Surface morphology

The surface morphology of the LCO particles before and after the PBNL coating was examined by scanning electron microscopy (SEM). Fig. 3 shows the LCO surface following one, three, five and nine successive PB nanolayer deposition cycles (1c, 3c, 5c and 9c) together with that of the uncoated LCO particles. The morphology is clearly different from that of the LCO surface in the absence of any PBNL coating treatment (Fig. 3a–j) – the surface of the uncoated LCO particles is smooth in contrast to the roughness characterizing the PBNL@LCO surface. Elemental mappings obtained by energy-dispersive X-ray spectroscopy (EDX) for PBNL9c@LCO are shown in Fig. 3k–n. The Fe atoms from the coating material, PB are homogeneously distributed over the entire surface area

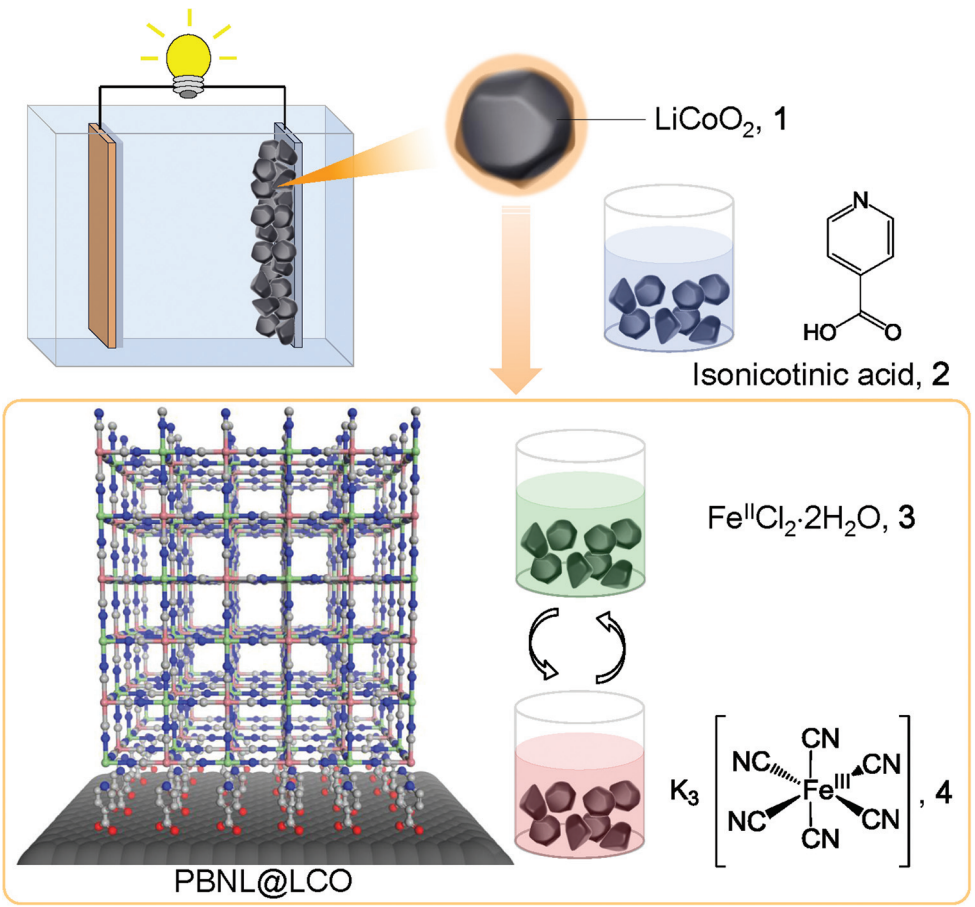

Fig. 1 Schematic illustration of the surface coating of $LiCoO_2$ with Prussian blue. $LiCoO_2$ (LCO) particles, **1** are immersed into an ethanol solution of isonicotinic acid, **2**. After rinsing excess physisorbed isonicotinic acid with ethanol, the LCO particles are alternately immersed into aqueous solutions of $FeCl_2{\cdot}4H_2O$, **3**, and $K_3[Fe(CN)_6]$, **4** including intermediate solvent (water) immersion and room temperature drying steps. This sequential step-by-step procedure results in the generation of PB-coated LCO particle surface (PBNL@LCO) of controllable thickness.

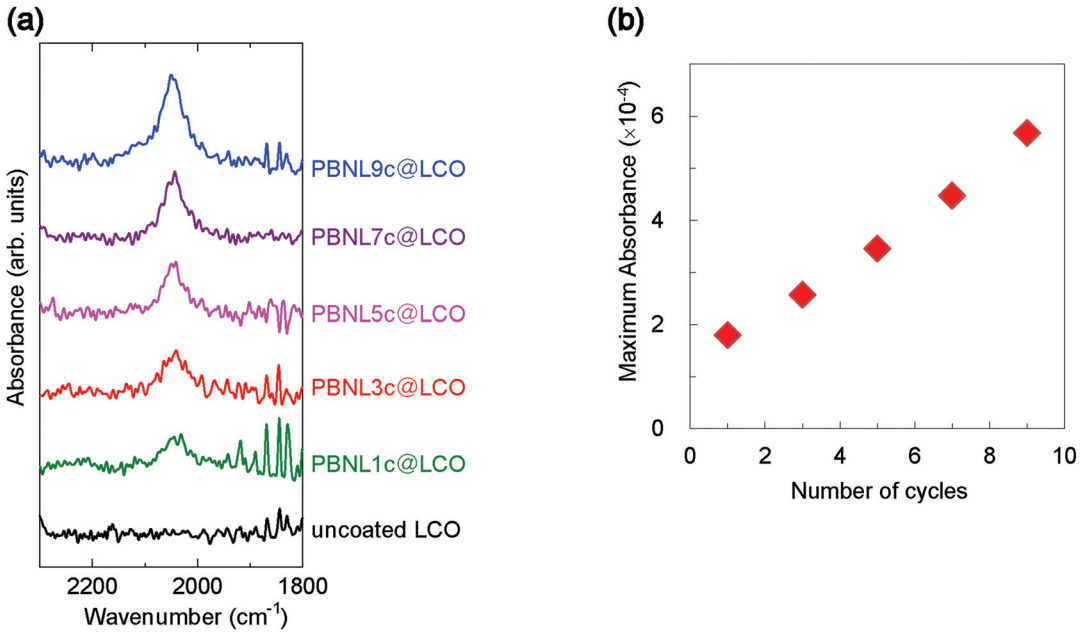

Fig. 2 Sequential growth of PBNL on LCO nanoparticles followed by infrared absorption spectroscopy. (a) Infrared (IR) absorption spectra of PBNL-coated LCO particles after successive cycles of solution immersion, rinsing, and drying. Each spectrum is labeled by the corresponding cycle number (1–9). (b) Plot of maximum absorbance of the T_{1u} stretching vibration of the bridging cyanide ions in PBNL at ~2050 cm^{-1} *versus* the number of PBNL growth cycles.

in the same way as the Co and O atoms from the LCO particles, confirming that PBNL is uniformly coated on the LCO surface.

Electrical properties

In order to examine the influence of the surface-coated PBNL on the LCO electrical properties, the resistivity of PBNL@LCO samples was measured by the impedance spectroscopy technique. Fig. 4a shows the complex impedance curves obtained from pellet-shaped samples of the LCO particles after one, three, and five cycles of the PBNL deposition treatment together with that of the uncoated LCO for comparison. The total resistance increases monotonically with the increasing number of coating cycles (Fig. 4a). The impedance spectra in Nyquist representation for uncoated LCO, PBNL1c@LCO, and PBNL3c@LCO comprise two semicircles with each spectrum containing three resistive components: the bulk resistance inside the LCO particles (R_0), the grain boundary resistance (R_1), and the contact resistance between LCO particles and the current collector (R_2), as shown in Fig. 4b. The evolution of the resistivity after taking into account the pellet area and thickness with the number of PBNL coating cycles is shown in Fig. 4c. R_1 and R_2 increase as the number of PBNL coating cycles increases. This implies that the coated PBNL is highly insulating as seen in its bulk state. On the other hand, R_0 remains the same as the LCO internal resistance is not affected by the surface coating. We note that it was not possible to extract R_1 from the impedance spectra of PBNL5c@LCO as the separation between the two semicircles was not clear (Fig. 4a). A high cell resistance generally causes lowering of the cell performance. Therefore, we selected PBNL1c@LCO and PBNL3c@LCO as the positive electrodes for cell application and examined the corresponding cell characteristics.

Electrochemical cell

Fig. 5 shows charge–discharge curves at a current density of 0.1 mA cm^{-1} for the electrochemical cells consisting of PBNL@LCO together with that of the uncoated LCO particles for comparison. A liquid electrolyte of 1 M $LiPF_6$ in ethylene carbonate–diethyl carbonate (EC–DEC) was used for the cells. SEM measurements of the PBNL@LCO particles before and after immersion for 90 hours into the liquid electrolyte (Fig. S1†) confirm that the surface morphologies do not change after immersion and the coated PBNL is stable in the liquid electrolyte employed. The cell of PBNL1c@LCO shows a discharge capacity of 130 mA h g^{-1} which is close to the specific capacity of LCO (~150 mA h g^{-1}).[16] On the other hand, the discharge capacity for the PBNL3c@LCO cell is 100 mA h g^{-1}, which is smaller than that of the referential uncoated LCO cell. This may be attributed to the large cell resistance caused by coating with insulating PBNL as revealed by the impedance measurements. The discharge curves for the PBNL1c@LCO and PBNL3c@LCO cells show a step at a cell potential of 3.2 V *vs.* Li which is smaller than that of the typical LCO cell potential (4.2 V *vs.* Li), but identical to the reported value for the cells composed of bulk PB as a positive electrode material.[7b] Therefore, we consider that the discharge capacity for the step part is from the coated PBNL.

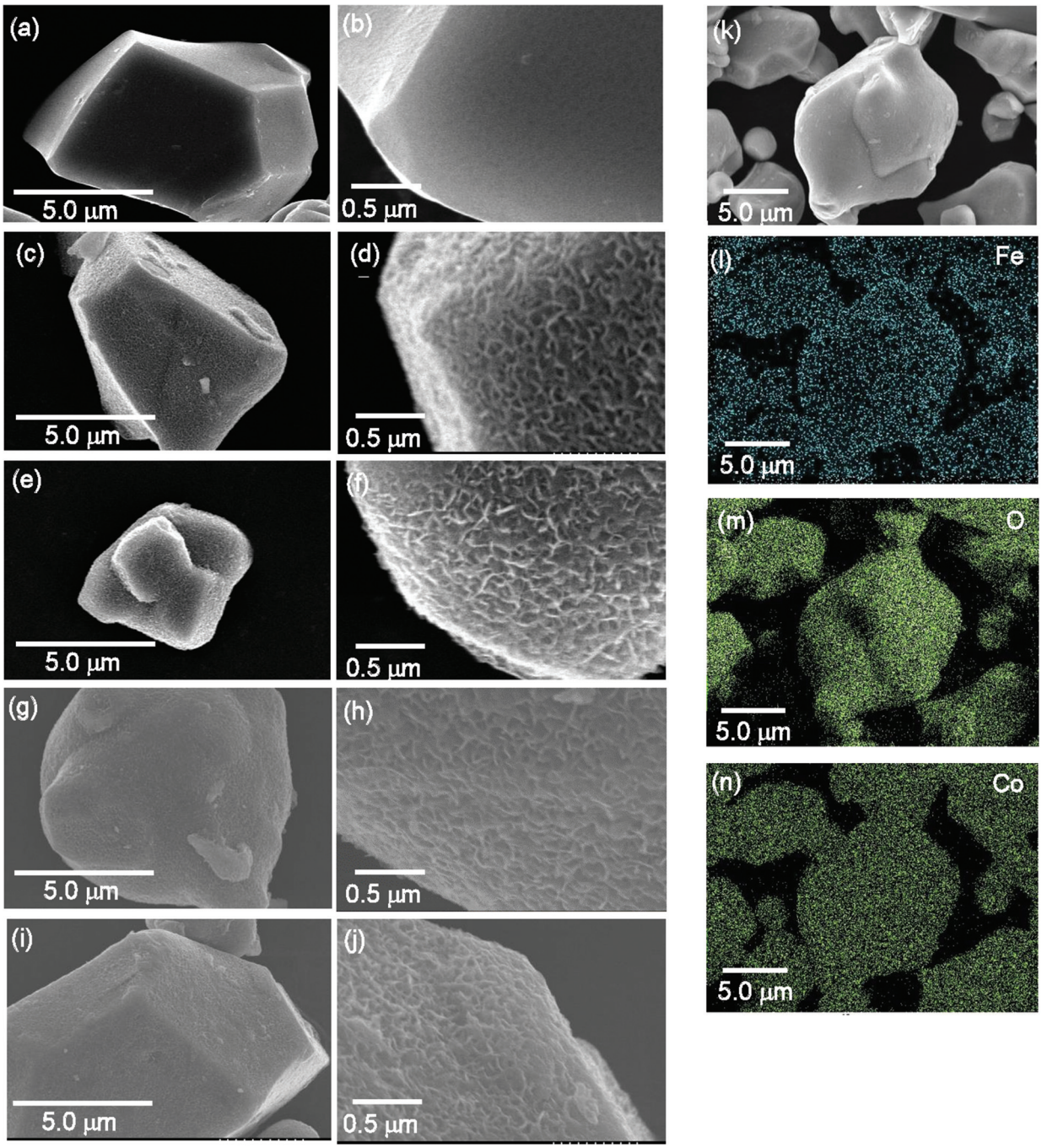

Fig. 3 Surface morphology and elemental analysis of PBNL@LCO. (a)–(j) Scanning electron microscopy (SEM) images of the uncoated LCO particles (a), (b) and the LCO particles following one, three, five and nine successive PB nanolayer deposition cycles (1c, 3c, 5c and 9c) – PBNL1c@LCO (c)/(d), PBNL3c@LCO (e)/(f), PBNL5c@LCO (g)/(h), and PBNL9c@LCO (i)/(j). (k)–(n) Elemental mappings obtained by energy-dispersive X-ray spectroscopy (EDX) for PBNL9c@LCO. Mapping elements are Fe (l) from PBNL and Co (m) and O (n) from LCO. The corresponding PBNL9c@LCO particle SEM image is shown in (k).

Conclusion

We have demonstrated a successful step-by-step modification of the surface of $LiCoO_2$ (LCO) particles with Prussian blue (PB) nanolayers by applying successive deposition cycles of immersion of the particles into solutions of $FeCl_2{\cdot}4H_2O$ and $K_3[Fe(CN)_6]$. IR spectroscopy revealed that the surface-coated PB nanolayers grow in a sequential manner. We confirmed the operation of electrochemical cells with PB-coated LCO particles as the positive electrode. In particular, the cells incorporated with the LCO particles after one cycle of PBNL deposition treatment shows a discharge capacity of 130 mA h g^{-1} which is

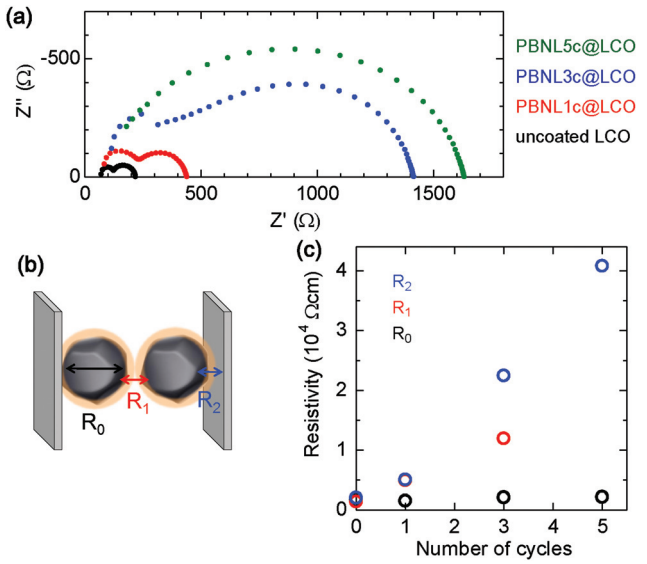

Fig. 4 Complex impedance curves for PBNL@LCO. (a) Impedance spectra in Nyquist representation obtained from pellet-shaped uncoated LCO (black dots), PBNL1c@LCO (red dots), PBNL3c@LCO (blue dots), and PBNL5c@LCO (green dots). (b) Schematic image of the resistive components: the bulk resistance inside the LCO particles (R_0), the grain boundary resistance (R_1), and the contact resistance between LCO and the current collector (R_2). (c) The evolution of the three components, R_0 (black circle), R_1 (red circle), and R_2 (blue circle) with the number of PBNL coating cycles. We note that it was not possible to extract R_1 from the impedance spectra of PBNL5c@LCO as the separation between the two semicircles was not clear.

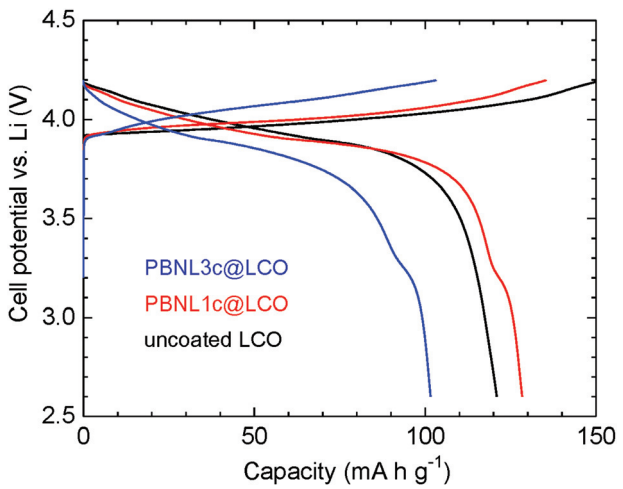

Fig. 5 The first charge–discharge curve for the electrochemical cells. Uncoated LCO (black line), PBNL1c@LCO (red line), and PBNL3c@LCO (blue line) are used as the positive electrode material. The constant specific current is 0.1 mA cm^{-1}.

close to the specific capacity of LCO (~150 mA h g^{-1}). We believe that the results presented here open a new direction for creating suitable interfacial conditions between electrode materials and electrolytes in secondary battery materials.

Acknowledgements

We thank Mr Shogo Matsui and Mrs Yuka Susami for technical support. We thank the Japan Science and Technology Agency (JST) "the Core Research for Evolutional Science and Technology (CREST)", "Advanced Low Carbon Technology Research and Development Program (ALCA)" and "Precursory Research for Embryonic Science and Technology (PRESTO)" for a project of "Molecular technology and creation of new functions", the Japan Society for the Promotion of Science (JSPS) "Grants-in-Aid for Scientific Research on Innovative Areas for Coordination Programming (22108524, 24108735)" and the Ministry of Education, Culture, Sports, Science and Technology (MEXT) "Special Coordination Funds (SCF) for Promoting Science and Technology".

References

1 (*a*) J.-M. Tarascon and M. Armand, *Nature*, 2001, **414**, 359; (*b*) M. S. Whittingham, *Chem. Rev.*, 2004, **104**, 4271; (*c*) F. Croce, G. B. Appetecchi, L. Persi and B. Scrosati, *Nature*, 1998, **394**, 456; (*d*) T. Minami, A. Hayashi and M. Tatsumisago, *Solid State Ionics*, 2006, **177**, 2715; (*e*) T. Niitani, M. Shimada, K. Kawamura and K. Kanamura, *J. Power Sources*, 2005, **146**, 386.

2 (*a*) K. Mizushima, P. C. Jones, P. J. Wiseman and J. B. Goodenough, *Mater. Res. Bull.*, 1980, **15**, 783; (*b*) J. N. Reimers and J. R. Dahn, *J. Electrochem. Soc.*, 1992, **139**, 2091.

3 (*a*) J. Cho, Y. J. Kim and B. Park, *Chem. Mater.*, 2000, **12**, 3788; (*b*) A. Basch and J. H. Albering, *J. Power Sources*, 2011, **196**, 3290; (*c*) G. T.-K. Fey, C.-Z. Lu, J.-D. Huang, T. P. Kumar and Y.-C. Chang, *J. Power Sources*, 2005, **146**, 65; (*d*) A. Sakuda, H. Kitaura, A. Hayashi, K. Tadanaga and M. Tatsumisago, *J. Electrochem. Soc.*, 2009, **156**, A27; (*e*) G. T.-K. Fey, Y. Y. Lin and T. P. Kumar, *Surf. Coat. Technol.*, 2005, **191**, 68; (*f*) J. Cho, Y. J. Kim, T.-J. Kim and B. Park, *Angew. Chem., Int. Ed.*, 2001, **40**, 3367; (*g*) H. J. Kweon, S. J. Kim and D. G. Park, *J. Power Sources*, 2000, **88**, 255; (*h*) T. Fang and J.-G. Duh, *Surf. Coat. Technol.*, 2006, **201**, 1886.

4 (*a*) A. Sakuda, T. Ohtomo, S. Hama, A. Hayashi and M. Tatsumisago, *J. Power Sources*, 2011, **196**, 6735; (*b*) A. Sakuda, A. Hayashi and M. Tatsumisago, *Sci. Rep.*, 2013, **3**, 2261; (*c*) S. Teragawa, K. Aso, K. Tadanaga, A. Hayashi and M. Tatsumisago, *Chem. Lett.*, 2013, **42**, 1435; (*d*) S. Teragawa, K. Aso, K. Tadanaga, A. Hayashi and M. Tatsumisago, *J. Power Sources*, 2014, **248**, 939; (*e*) S. Teragawa, K. Aso, K. Tadanaga, A. Hayashi and M. Tatsumisago, *J. Mater. Chem. A*, 2014, **2**, 5095.

5 (*a*) S. Kitagawa, R. Kitaura and S. Noro, *Angew. Chem., Int. Ed.*, 2004, **43**, 2334; (*b*) H.-C. Zhou, J. R. Long and O. M. Yaghi, *Chem. Rev.*, 2012, **112**, 673; (*c*) G. Ferey, *Chem. Soc. Rev.*, 2008, **37**, 191; (*d*) B. Liu, M. Tu, D. Zacher and R. A. Fischer, *Adv. Funct. Mater.*, 2013, **23**, 3790;

(*e*) T. R. Cook, Y.-R. Zheng and P. J. Stang, *Chem. Rev.*, 2013, **113**, 734.

6 (*a*) H. J. Buser, D. Schwarzenbach, W. Petter and A. Ludi, *Inorg. Chem.*, 1977, **16**, 2704; (*b*) M. Ohba and H. Okawa, *Coord. Chem. Rev.*, 2000, **198**, 313; (*c*) M. P. Shores, L. G. Beauvais and J. R. Long, *J. Am. Chem. Soc.*, 1999, **121**, 775; (*d*) D. Papanikolaou, S. Margadonna, W. Kosaka, S.-I. Ohkoshi, M. Brunelli and K. Prassides, *J. Am. Chem. Soc.*, 2006, **128**, 8358; (*e*) O. Sato, T. Iyoda, A. Fujishima and K. Hashimoto, *Science*, 1996, **272**, 704; (*f*) H. Tokoro and S.-I. Ohkoshi, *Dalton Trans.*, 2011, **40**, 6825; (*g*) S.-I. Ohkoshi, K. Nakagawa, K. Tomono, K. Imoto, Y. Tsunobuchi and H. Tokoro, *J. Am. Chem. Soc.*, 2010, **132**, 6620; (*h*) S. Ferlay, T. Mallah, R. Ouahès, P. Veillet and M. Verdaguer, *Nature*, 1995, **378**, 701; (*i*) T. Mallah, S. Thiebaut, M. Verdaguer and P. Veillet, *Science*, 1993, **262**, 1554.

7 (*a*) N. Imanishi, T. Morikawa, J. Kondo, Y. Takeda, O. Yamamoto, N. Kinugasa and T. Yamagishi, *J. Power Sources*, 1999, **79**, 215; (*b*) D. Asakura, C. H. Li, Y. Mizuno, M. Okubo, H. Zhou and D. R. Talham, *J. Am. Chem. Soc.*, 2013, **135**, 2793; (*c*) Y. Mizuno, M. Okubo, E. Hosono, T. Kudo, H. Zhou and K. Oh-Ishi, *J. Phys. Chem. C*, 2013, **117**, 10877; (*d*) M. Okubo and I. Honma, *Dalton Trans.*, 2013, **42**, 15881; (*e*) M. Takachi, T. Matsuda and Y. Moritomo, *Jpn. J. Appl. Phys.*, 2013, **52**, 044301; (*f*) R. Y. Wang, C. D. Wessells, R. A. Huggins and Y. Cui, *Nano Lett.*, 2013, **13**, 5748; (*g*) S.-H. Yu, M. Shokouhimehr, T. Hyeon and Y.-E. Sung, *ECS Electrochem. Lett.*, 2013, **2**, A39; (*h*) P. Nie, L. Shen, H. Luo, B. Ding, G. Xu, J. Wang and X. Zhang, *J. Mater. Chem. A*, 2014, **2**, 5852; (*i*) T. Matsuda and Y. Moritomo, *Appl. Phys. Express*, 2011, **4**, 047101.

8 (*a*) J. T. Culp, J.-H. Park, I. O. Benitez, Y.-D. Huh, M. W. Meisel and D. R. Talham, *Chem. Mater.*, 2003, **15**, 3431; (*b*) M. Pyrasch, A. Toutianoush, W. Jin, J. Schnepf and B. Tieke, *Chem. Mater.*, 2003, **15**, 245; (*c*) D. R. Talham and M. W. Meisel, *Chem. Soc. Rev.*, 2011, **40**, 3356; (*d*) D. M. Pajerqwski, M. J. Andrus, J. E. Gardner, E. S. Knowles, M. W. Melsel and D. R. Talham, *J. Am. Chem. Soc.*, 2010, **132**, 4058; (*e*) S. Tricard, Y. Raza, S. Mazerat, K. Aissou, T. Baron and T. Mallah, *Dalton Trans.*, 2013, **42**, 8034; (*f*) S. Tricard, F. Charra and T. Mallah, *Dalton Trans.*, 2013, **42**, 15835; (*g*) S. Tricard, B. Fleury, F. Volatron, C. Costa-Coquelard, S. Mazerat, V. Huc, C. David, F. Brisset, F. Miserque, P. Jegou, S. Palacin and T. Mallah, *Chem. Commun.*, 2010, **46**, 4327.

9 (*a*) O. Shekhah, H. Wang, S. Kowarik, F. Schreiber, M. Paulus, M. Tolan, C. Sternemann, F. Evers, D. Zacher, R. A. Fischer and C. Wöll, *J. Am. Chem. Soc.*, 2007, **129**, 15118; (*b*) O. Shekhah, H. Wang, T. Strunskus, P. Cyganik, D. Zacher, R. Fischer and C. Wöll, *Langmuir*, 2007, **23**, 7440; (*c*) D. Zacher, R. Schmid, C. Wöll and R. A. Fischer, *Angew. Chem., Int. Ed.*, 2011, **50**, 176; (*d*) R. Makiura, S. Motoyama, Y. Umemura, H. Yamanaka, O. Sakata and H. Kitagawa, *Nat. Mater.*, 2010, **9**, 565; (*e*) R. Makiura, K. Tsuchiyama and O. Sakata, *CrystEngComm*, 2011, **13**, 5538; (*f*) R. Makiura and O. Konovalov, *Dalton Trans.*, 2013, **42**, 15931; (*g*) R. Makiura and O. Konovalov, *Sci. Rep.*, 2013, **3**, 2506; (*h*) R. Makiura, R. Usui, Y. Sakai, A. Nomoto, A. Ogawa, O. Sakata and A. Fujiwara, *ChemPlusChem*, 2014, **79**, 1352.

10 G. Lu, S. Li, Z. Guo, O. K. Farha, B. G. Hauser, X. Qi, Y. Wang, X. Wang, S. Han, X. Liu, J. S. Duchene, H. Zhang, Q. Zhang, X. Chen, J. Ma, S. C. J. Loo, W. D. Wei, Y. Yang, J. T. Hupp and F. Huo, *Nat. Chem.*, 2012, **4**, 310.

11 P. Falcaro, F. Normandin, M. Takahashi, P. Scopece, H. Amenitsch, S. Costacurta, C. M. Doherty, J. S. Laird, M. D. H. Lay, F. Lisi, A. J. Hill and D. Buso, *Adv. Mater.*, 2011, **23**, 3901.

12 S. Sorribas, B. Zornoza, C. Téllez and J. Coronas, *Chem. Commun.*, 2012, **48**, 9388.

13 (*a*) T. Zhang, X. Zhang, X. Yan, L. Kong, G. Zhang, H. Liu, J. Qiu and K. L. Yeung, *Chem. Eng. J.*, 2013, **228**, 398; (*b*) M. E. Silvestre, M. Franzreb, P. G. Weidler, O. Shekhah and C. Wöll, *Adv. Funct. Mater.*, 2013, **23**, 1210.

14 P. Falcaro, A. J. Hill, K. M. Nairn, J. Jasieniak, J. I. Mardel, T. J. Bastow, S. C. Mayo, M. Gimona, D. Gomez, H. J. Whitfield, R. Riccò, A. Patelli, B. Marmiroli, H. Amenitsch, T. Colson, L. Villanova and D. Buso, *Nat. Commun.*, 2011, **2**, A237.

15 R. Ricco, L. Malfatti, M. Takahashi, A. J. Hill and P. Falcaro, *J. Mater. Chem. A*, 2013, **1**, 13033.

16 R. Koksbang, J. Barker, H. Shi and M. Y. Saïdim, *Solid State Ionics*, 1996, **84**, 1.